



Accurate measurements of phase refractive index of soft contact lenses

TODD SZARLAN,¹ DONALD GIBSON,² XIN WEI,¹ AND FILIPP IGNATOVICH^{2,*}

¹Johnson & Johnson Vision Care, 7500 Centurion Parkway, Jacksonville, FL 32256, USA

²Lumetrics Inc, 1565 Jefferson Rd, #420, Rochester, NY 14623, USA

*fignatovich@lumetrics.com

Abstract: We describe a measurement approach for the bulk phase refractive index of hydrogel and silicone hydrogel (soft) contact lenses in solution at multiple wavelengths with an accuracy of ± 0.001 , and sensitivity to change of 0.0002. The method uses time-domain low-coherence interferometry to obtain group refractive index (GRI) for contact lenses between 530 to 670 nm in 10 nm increments. The measured GRI dispersion curve is then mathematically converted to the phase refractive index values. The approach is based on a point measurement using focused beam, and therefore does not require flattening of the lens for the measurements. We discuss practical implications of the method for the quality control in manufacturing of ophthalmic optics.

© 2020 Optical Society of America under the terms of the [OSA Open Access Publishing Agreement](#)

1. Introduction

Soft contact lenses are made using hydrogel and silicon hydrogel materials. The lenses are manufactured by UV curing polymers inside molds, hydrated, and packaged into a saline solution before being shipped to the customer. During the quality control process, a percentage of the lenses are removed from the manufacturing line and evaluated in the laboratory, where the optical properties of the lens are measured using interferometric or other methods. During these measurements, the lens is held inside a cuvette filled with liquid, and therefore only the in-liquid measurements are conducted. In order to properly qualify the optical properties of the lens during use, the in-liquid performance must be converted into in-air (in-situ) performance. The conversion equation depends on the phase refractive index (RI) of the lens material and is highly sensitive to changes in the RI at the low 4th decimal place.

The Abbe refractometer has been the gold standard for material phase refractive index measurements and is broadly utilized for measuring the RI of contact lenses. In this instrument, the lens is sandwiched between two prisms and illuminated with a monochromatic source. The incident light is refracted at the lens material/prism interface and the divergent critical angle determined. With the knowledge of the prism refractive index and the measured angle, Snell's Law is used to calculate the refractive index.

Despite its proven general track record, the Abbe refractometer is associated with a number of problems when applied to measuring the RI of soft contact lenses:

- The measurements are done at the surface rather than in the bulk of the material,
- The measurement is typically performed at 589 nm (sodium D line) and requires a conversion to the wavelength used in the interferometer (e.g. 543 nm),
- The lens is deformed (flattened) creating stresses in the material,
- Squeezing the lens between the prisms modifies the water content of the lens affecting its properties.

Manufacturers put a lot of effort in controlling errors associated with these issues. However, even with those controls in place, complex lens chemistry of some materials leads to measurement

variations larger than the threshold value of ± 0.005 set by the ISO 18369 contact lens requirement [1]. It is a source of continuous difficulty for contact lens manufacturers, and significant efforts have been put in place to overcome these issues.

In the past, a method has been developed by JJVC in collaboration with the University of Arizona, aimed at obtaining accurate phase RI measurements [2]. This method requires flattening of the lens for measurements. Ultimately, due to its complexity, this method could not be effectively utilized outside of the research laboratory.

In this article we describe an alternative method that uses recent advances in supercontinuum light generation, enabling highly accurate measurements of *group* refractive index (GRI) at multiple wavelengths [3]. The GRI dispersion curve is then converted into the phase RI values [4]. The developed conversion approach and procedure enables the target phase RI error of below ± 0.001 for the limited (but practical) range of the refractive index values.

The measurement technique described here represents a variation of the technique based on combining the low-coherence interferometer (LCI) and confocal scanning measurement modalities [5,6,7]. The combined technique has been successfully demonstrated in obtaining phase refractive indices of materials with the accuracy of down to 0.0001. The combined technique was shown to work well for glass materials above 1mm in thickness measured in air. The technique in general was difficult to apply for thinner samples, where the measurement error increases significantly for samples below 300 microns. A contact lens is typically a 70-300 microns layer of soft hydrogel material with high water content when placed in saline. It therefore represents a challenging thin sample, having also low optical reflectivity from its interfaces as compared to glass-air interfaces. The technique described here is based on using a single measurement modality (LCI), which eliminates errors and challenges associated with using an additional confocal measurement modality on a thin sample. It therefore represents a simpler technique that may find utility outside of the laboratory environment as we discuss in Section 5.

2. Measurement system description

Figure 1 shows the measurement configuration. The motorized translation stage (9) contains two mirrors that act as a reference arm for two interferometers – a laser interferometer for displacement measurements, and the time-domain low-coherence interferometer. The LCI utilizes a tunable super-continuum light source (SCLS) (1) to select different measurement wavelengths. A balanced detector (8) is utilized to reduce the power noise. Polarization optics (3) and (4) are used to achieve balanced detection by taking advantage of the reflection of the returning light from the beamsplitter cube (5), that otherwise is lost in a standard Michelson configuration.

The physics of low-coherence interferometry or partial-coherence interferometry is extensively covered in literature [8,9]. Here we use a time-domain variation of LCI [10]. In short, during the motion of the translation stage, when the reference arm length becomes equal to the distance from the beam splitting cube (5) to a reflecting surface within the sample, the output of the balanced detector oscillates due to the interference. These bursts of oscillations are present for all reflecting surfaces in the sample. The distance that the translation stage travels between the interferometric signal bursts is then equal to the *optical* distance (physical distance times the group refractive index) between the corresponding reflecting surfaces within the sample. Typically, the envelope of these interferometric oscillations is plotted [see Fig. 2(d)]. The LCI and its variations are the primary engine behind optical coherence tomography [11], as well as the go-to method for non-contact material thickness measurement applications [12,13].

The width of the signal peaks in Fig. 2(d) is equal to the coherence length of the light source, which is inversely proportional to its spectral bandwidth. The coherence length specifies the thinnest possible optical thickness that can be measured using LCI. The tunable filter (1) limits the spectral bandwidth of the SCLS to 10 nm for each measurement. Such spectral bandwidth

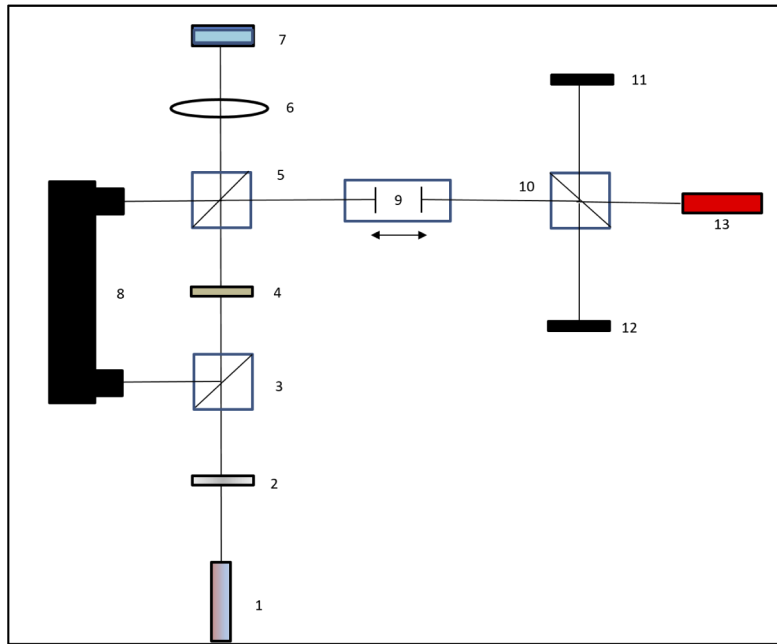


Fig. 1. Measurement configuration (Marcus, Gibson, Hadcock, & Ignatovich, 2019). (1) Super-continuum light source (NKT SUPERK Extreme) with tunable filter (SUPERK VARIA), (2) neutral density filter, (3) polarizing beam splitter cube (Thorlabs CCM1-PBS251), (4) superachromatic quarter waveplate (Thorlabs SAQWP05M-700), (5) & (10) 50/50 beam splitter cubes (CCM1-BS013), (6) focusing lens, (7) measurement cuvette & sample, (8) large-area balanced photodetector (Thorlabs PDB210A), (9) motorized translation stage with optics (NPN ST100050QN linear motor stage). (10-13) laser interferometer used for measuring the displacement of the translation stage, (11) mirror, (12) photodetector (Thorlabs PDA10A), (13) helium neon laser (Thorlabs HNLS008R).

corresponds to approximately 50 μm coherence length of the filtered light source and is sufficiently narrow to allow measurements of most contact lenses.

A laser interferometer (10-13) is used to track position of the translation stage and for data acquisition. The signal oscillations from the laser detector are used to generate the data acquisition clock pulses using zero-crossing electronics. The clock pulses are then used to digitize the envelope of the LCI interferometric signal of the low-coherence interferometer. This approach results in an array of equidistant data points, which are then used to calculate optical distances between the reflecting surfaces of the sample [14].

2.1. GRI measurement approach

LCI is used to measured optical distances between the reflecting surfaces of the sample. The physical thickness is calculated by dividing the measured optical distance by the group refractive index of the corresponding material. Inversely, the GRI can be calculated if both physical and optical thicknesses are known.

Physical thickness of an unknown object can also be obtained using LCI, by placing it between two walls of a glass cuvette. Then, the distance between the walls of the cuvette, and the distances between the walls and the object can be measured in air. The refractive index of air is well characterized and known from previous studies and is close to 1 with a high degree of precision [15].

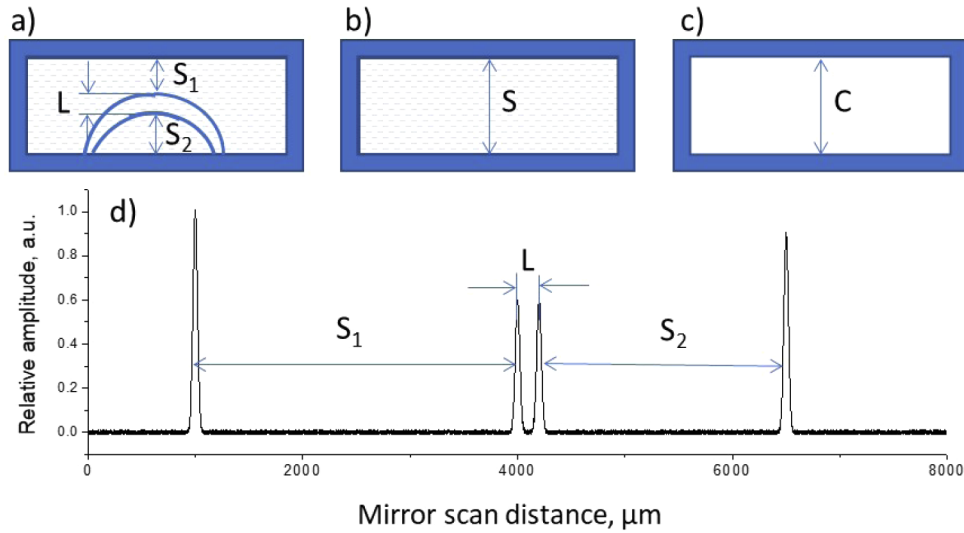


Fig. 2. Schematic representation of the three steps used for measuring GRI of the contact lens. See Eq. (1). a) Step 1: contact lens inside the cuvette filled with liquid, and the corresponding optical distances. The schematic is not to scale. b) Step 2: optical thickness of the cuvette filled with saline. c) Step 3: Optical thickness of the empty cuvette. d) Illustration of the low-coherence interferometric signal (the envelope of the interferometric oscillations) that correspond to the contact lens located inside the cuvette.

Measuring physical thickness of a contact lens requires additional steps as the lens must be hydrated. Therefore, for the purposes of GRI measurements, the following 3-step approach is used:

1. Glass cuvette is filled with a solution and the contact lens is placed inside the cuvette. LCI is used to measure optical distances between the walls of the cuvette and the contact lens, S_1 and S_2 , and the optical thickness of the contact lens, L [Fig. 2(a)].
2. The lens is removed from the cuvette, and the optical thickness of the cuvette with solution, S , is measured [Fig. 2(b)].
3. The solution is evacuated from the cuvette, and the optical thickness of the empty cuvette, C , is measured [Fig. 2(c)].

After completing the 3-step process, the GRI of the lens is calculated using the following equation:

$$n_l = n_a \cdot \frac{S}{C} \cdot \frac{L}{(S - S_1 - S_2)} \quad (1)$$

where n_a and n_l are the GRIs for the air and for the lens respectively.

The above measurement procedure is repeated for every wavelength as the filter is stepped every 10 nm between 530 nm to 670 nm. At the end of the measurement an array of 15 GRI values at 15 different wavelengths is obtained for the contact lens. We refer to this data array as the GRI dispersion curve.

2.2. Phase refractive index conversion approach

The approach for converting the GRI dispersion curve to the phase refractive index is based on previous work [4]. According to that study, both the phase index (n) and the group index (n_g) can

be expressed in similar forms:

$$n = p_0 + p_1\omega + p_2\omega^2 \quad (2)$$

$$n_g = p_0 + p_1x + p_2y \quad (3)$$

where x and y are

$$x = \frac{\lambda^* \omega^2 - 2\lambda_0\omega + \lambda_0}{\lambda^* - \lambda_0} \quad (4)$$

$$y = \frac{2\lambda^* \omega^3 - (\lambda^* + 3\lambda_0)\omega^3 + 2\lambda_0 \omega}{\lambda^* - \lambda_0} \quad (5)$$

and ω a function of λ , with λ^* and λ_0 constants,

$$\omega = \frac{\lambda - \lambda_0}{\lambda - \lambda^*} \quad (6)$$

Parameters λ^* and λ_0 are used in the chromatic coordinates formalism in aberration theory [16,17] and adopted to convert group refractive index into phase refractive index [4]. Both parameters act as fitting variables – if we assume certain values for constants λ^* and λ_0 , and measure n_g at three different wavelengths, we end up with a system of three linear equations that we can solve to obtain p_0 , p_1 , and p_2 . Once we know p_0 , p_1 , and p_2 , the phase index can be easily obtained at any wavelength. If more than three measurements of n_g are available, the data is fit with the dispersion formula obtained from the Sellmeier equation [18] to increase the overall accuracy. Materials of known and well characterized phase RI are then used to obtain proper values for parameters λ^* and λ_0 , that can then be applied to finding the phase RI for other materials, as described in the following section.

3. Calibration of the conversion constant λ^*

The main difficulty of applying the above GRI to phase RI conversion method lies in finding the right constants λ^* and λ_0 . We have found that λ_0 has very minor effect on the calculated values of the RI, therefore according to the approach taken in [4], λ_0 was chosen as 480 nm, “so that ω ranges roughly symmetrically over the visible spectrum”.

Value of λ^* is chosen (calibrated) to minimize the polynomial fit error using three materials with well-known and characterized refractive indices: DI water [19], fused silica [20] and BK-7 [21]. For each of these materials, the phase RI was obtained using the method described above, where the GRI dispersion curve was measured and converted to the phase RI values at 15 different wavelengths. The value of λ^* for calculations is chosen to minimize the error between the calculated and published RI values for each material. The known values of λ^* are plotted and fitted with a linear curve (Fig. 3).

The λ^* calibration also corrects any errors in the measured GRI values as compared to published values. For example, it is known (and we have observed) that the spectral content, such as the spectral bandwidth, of the measurement light affects the measured GRI value at each wavelength. This calibration technique therefore also addresses any variations due to using another light source (for example if a second such system is constructed, even if it is using the same type of the light source).

The linear curve in Fig. 3 is used to create a look-up table for determining the appropriate λ^* value for a given estimated phase RI value.

3.1. Prior knowledge of the material

During the conversion from GRI to phase RI, the calibration lookup table for λ^* is used to select the proper value for phase conversion. This implies that some knowledge of the material RI is required – for JJVC etafilcon materials, this value is typically 1.400 at 589 nm. To assess the

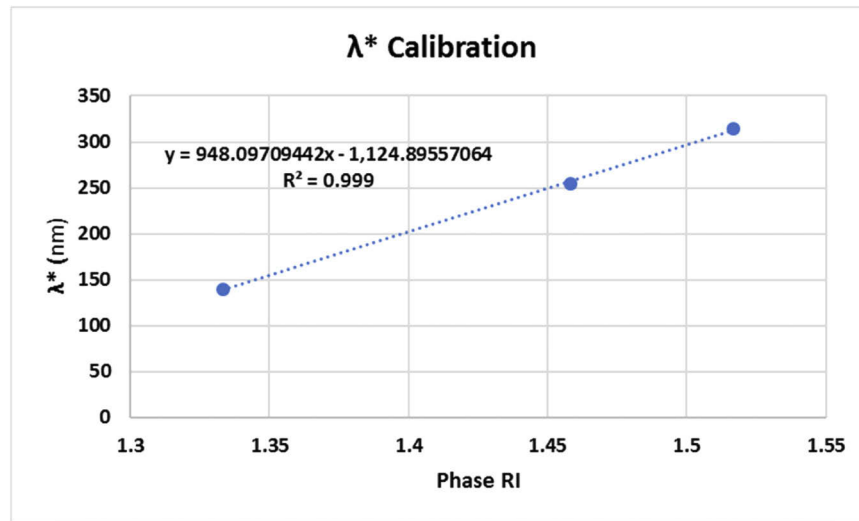


Fig. 3. Values of λ^* that minimize the deviation between the published and measured RI values for DI water, fused silica, and BK7. The linear fit is then used for choosing the proper λ^* when measuring the RI for other materials - some prior knowledge of the measured material is therefore required for accurate measurement results.

error in the conversion process due to the uncertainty in the prior knowledge, we have conducted a sensitivity study where different λ^* values were used in the conversion procedure for contact lenses. From this testing it was discovered that the needed accuracy of knowing the value λ^* is approximately 10%. For example, if contact lenses that were assumed to have an RI value of 1.400 were converted from group to phase index with λ^* values with a range of ~20nm (corresponding to assumed RI values of 1.39 to 1.41), the difference in the final phase RI values was ± 0.0001 . Running the same conversion for lenses at an assumed 1.420 RI value induced an error of ± 0.0002 . While λ^* is a critical component to proper group to phase conversion, it is not very sensitive when looking over small refractive index ranges. For typical JJVC contact lens materials, the initial estimate of λ^* based on material constituent components is precise enough to provide converted phase RI values in the ± 0.001 range.

4. Measurement data and results

4.1. Measurements of the GRI dispersion curve for different materials

Figure 4 thru Fig. 10 show the measured GRI values for multiple JJVC lens materials and for materials used as standards for λ^* . The data is obtained at different times and for different lenses. The graphs are presented as the mean measured value at each wavelength along with the 95% confidence interval around the measured values.

With the measured GRI repeatability standard deviation at the ~0.0004 level, the instrument can differentiate between contact lens materials and material batches, detect differences in contact lens raw material boundary (tolerance) conditions, identify changes due to stabilization post-manufacturing, and adequately measure known materials to be used as calibration/verification standards.

Development of the prototype instrument required controlling number of sources of errors – temperature influences, lens settling and stabilization times, external vibration, balanced detector channel equalization with wavelength, and SCLS spectral stability. Reducing or eliminating these sources of error led to individual optical path length measurement repeatability (standard

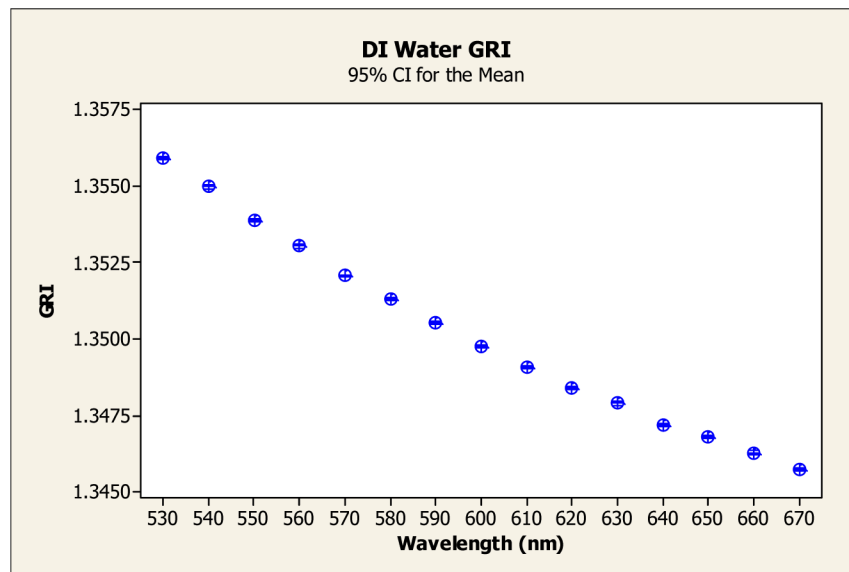


Fig. 4. DI water GRI dispersion curve, 12 measurements.

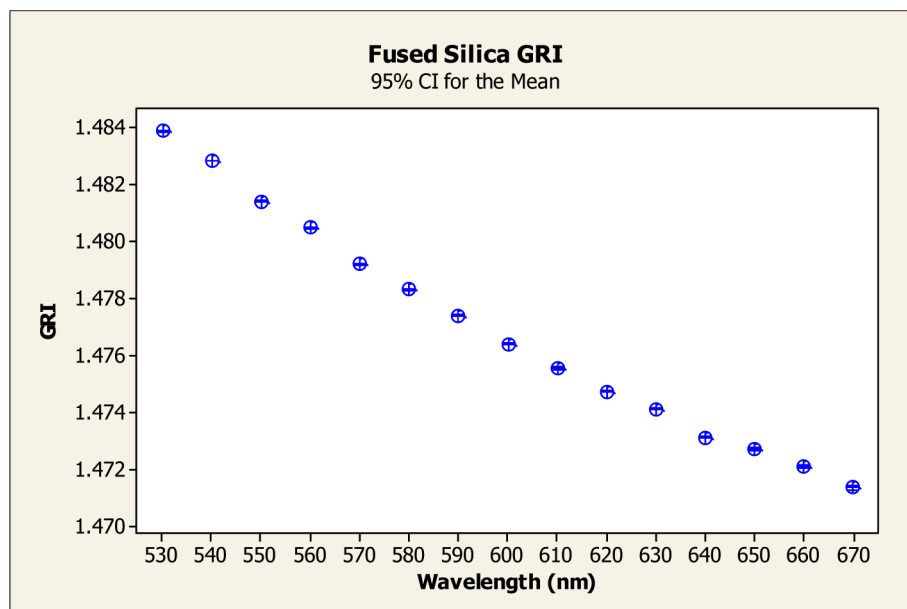


Fig. 5. Fused silica GRI dispersion curve, 12 measurements.

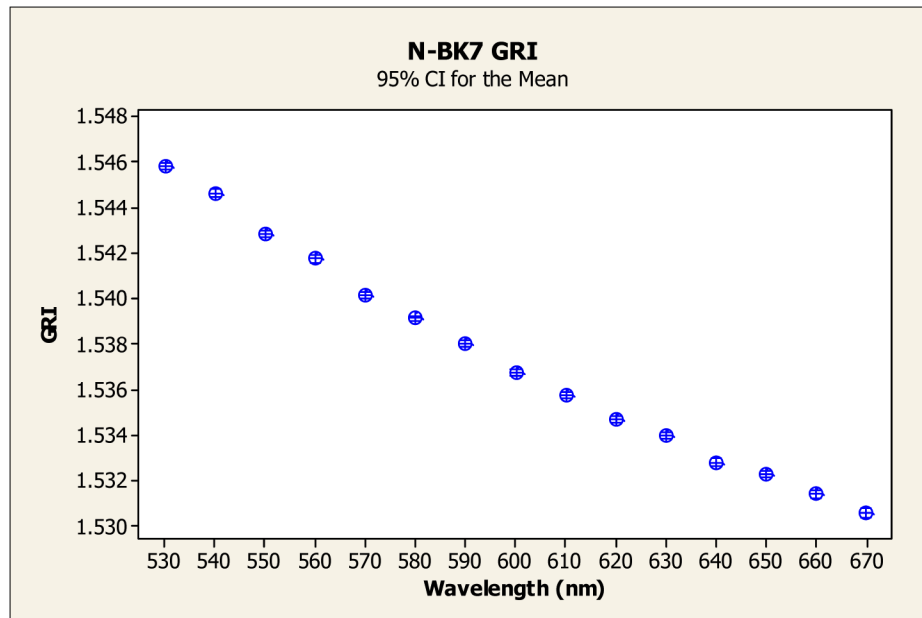


Fig. 6. N-BK7 GRI dispersion curve, 12 measurements.

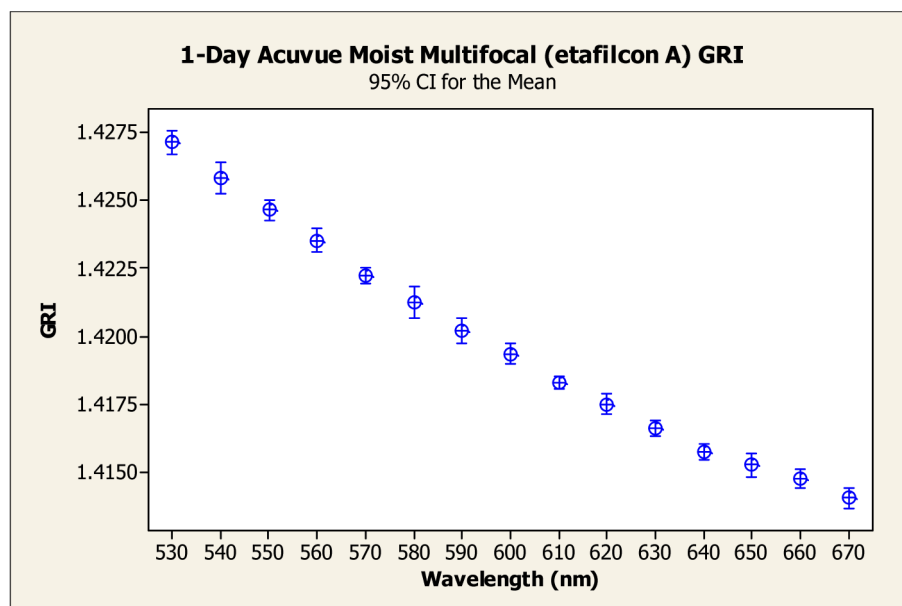


Fig. 7. 1-Day Acuvue moist multifocal GRI dispersion curve, 5 lenses.

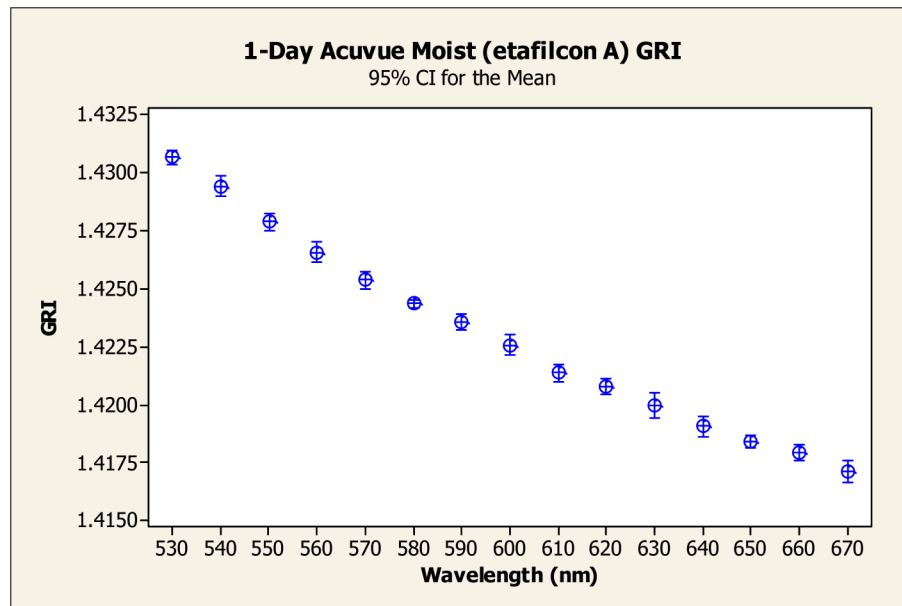


Fig. 8. 1-Day Acuvue moist GRI dispersion curve, 5 lenses.

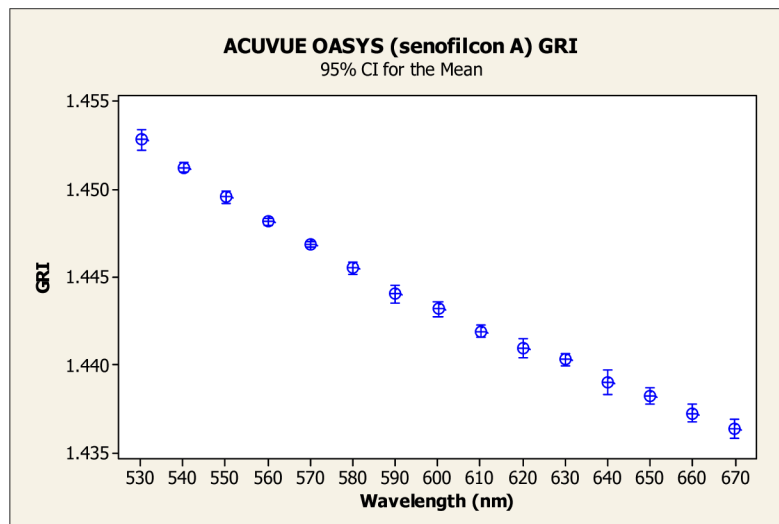


Fig. 9. Acuvue Oasis GRI dispersion curve, 5 lenses.

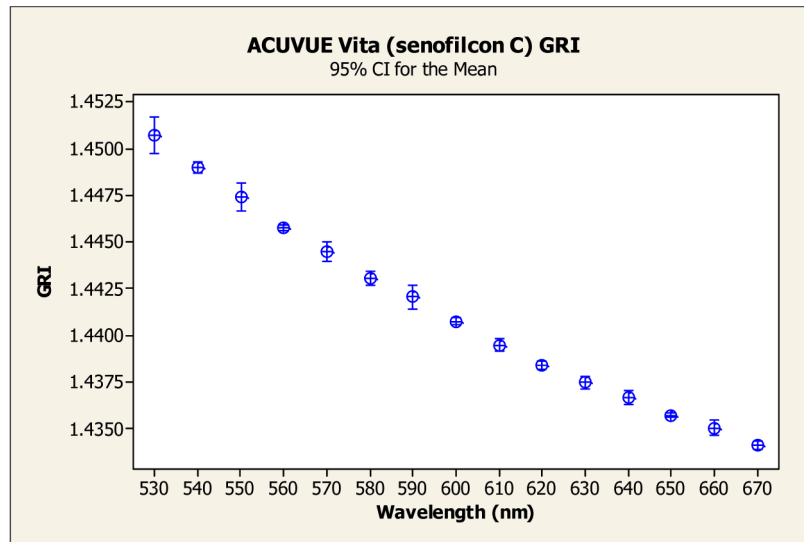


Fig. 10. Acuvue Vita GRI dispersion curve, 5 lenses.

deviation of 20 repeat measures) of < 200 nm, and GRI repeatability of ~ 0.0004 across all wavelengths. Table 1 provides a measurement example for the five optical distance parameters used to calculate the GRI of a contact lens at 540 nm, with the standard deviation and the average values calculated based on 20 consecutive measurements for each parameter.

Table 1. Summary of standard deviations of individual optical thickness measurements at 540 nm. These measurements are used in Eq. (1) to calculate GRI of the contact lens. All data is presented in micrometers.

	S	S_1	L	S_2	C
Std Dev	0.084	0.164	0.126	0.181	0.097
Average	6984.305	1049.572	281.583	5667.28	5146.487

The GRI measurement technique described above requires approximately 30 minutes per lens, with no single measurement element taking longer than another – it is simply the act of manually changing system settings across 45 individual measurements (3 measurement sets at 15 individual wavelengths). Adding in lens stabilization time and phase RI data processing, a typical lot of 5 lenses requires approximately 3.5 hours to complete.

4.2. Measurement accuracy of Phase RI

Measurement accuracy is evaluated for materials with known or accurately measurable phase RI values, by comparing these values to the phase RIs obtained using the GRI approach.

4.2.1. Glycerol

Glycerol is one of the readily available well-characterized liquids in 1.4 RI range. The literature contains data for Glycerol from 589 nm and up, with the phase RI around 1.47 range [22]. The GRI of the material was measured, converted to phase index using the appropriate λ^* value obtained from Fig. 3 for 1.47, and compared to the published values (Fig. 11 and Fig. 12). The data indicates the agreement to below 0.0007 for the wavelength range.

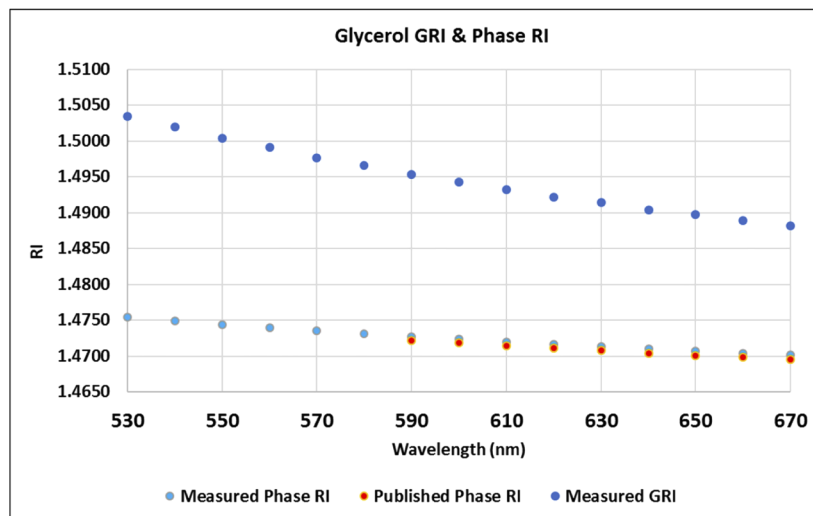


Fig. 11. Glycerol GRI & phase RI.

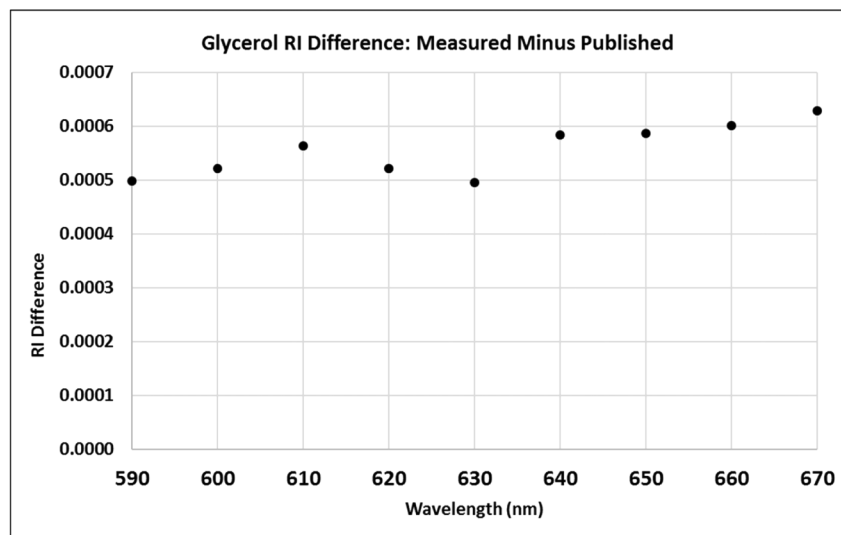


Fig. 12. Glycerol measured minus published phase RI.

4.2.2. Brix Sucrose

Brix sucrose is another well-characterized liquid, that can additionally be modified by changing the solution concentration. We use concentrations of 20%, 40% and 60%. These three concentrations correspond to phase refractive index values of 1.36384, 1.39986, and 1.44193 at 589.3 nm (sodium D line). The standards were first measured on a commercial Schmidt-Haensch refractometer (SHR) [23] at five wavelengths: 543.4, 546.1, 587.9, 589.3 and 656.3 nm. The same solutions were then measured using the GRI technique. The obtained phase RI dispersion curve was fit with a 2nd order polynomial to obtain values at the wavelengths used for SHR measurements. Table 2 shows the comparison data.

Table 2. Comparison of the phase RI obtained for three difference concentrations of Brix Sucrose using Schmidt-Haensch refractometer, and the GRI method.

Solution	Wavelength (nm)	RI Proposed	RI Schmidt_Haensch	Difference RI (Proposed - SH)	Certified RI Value	Difference Certified - SH	Difference Certified - Proposed
Brix 20%	543.4	1.36635	1.36559	0.00076			
	546.1	1.36625	1.36548	0.00076			
	587.6	1.36482	1.36395	0.00088			
	589.3	1.36477	1.36389	0.00088	1.36384	0.00005	0.00093
	656.3	1.36297	1.36191	0.00106			
Brix 40%	543.4	1.40221	1.40179	0.00042			
	546.1	1.40210	1.40168	0.00042			
	587.6	1.40058	1.40003	0.00054			
	589.3	1.40052	1.39997	0.00055	1.39986	0.00011	0.00066
	656.3	1.39860	1.39785	0.00075			
Brix 60%	543.4	1.44457	1.44398	0.00058			
	546.1	1.44445	1.44386	0.00059			
	587.6	1.44283	1.44209	0.00074			
	589.3	1.44277	1.44203	0.00074	1.44193	0.00010	0.00084
	656.3	1.44074	1.43977	0.00097			
			Average RI Δ	0.00071			

The SHR measurements agree with the certified values of the standards at the 0.0001 level at 589.3 nm. When comparing the GRI-based data to the SHR measured values, the average RI bias across all five wavelengths and three concentrations was 0.0007. The maximum RI bias was 0.001: for the 656.3 nm wavelength and 20% solution.

4.2.3. Etafilcon A at 589 nm

For some of the JJVC lenses, which are manufactured using etafilcon A, the Abbe refractometer has been shown to produce accurate results due to favorable lens chemistry. Table 3 shows the comparison data between the measurements obtained using the described GRI technique and using the Abbe refractometer. For each measurement, five different lenses from a given design/monomer batch were measured for GRI and converted to phase RI. The same lenses were then measured using the Abbe refractometer.

Table 3. GRI-based measurements vs Abbe measurements at 589 nm.

Design	Material	Measured Phase RI	Abbe Phase RI	RI Difference (Measured minus Abbe)
Multifocal	etafilcon A	1.4015	1.401	0.0005
Multifocal	etafilcon A	1.3993	1.400	-0.0007
Sphere	etafilcon A	1.4021	1.398	0.0041
Sphere	etafilcon A	1.4020	1.401	0.0010

As can be seen from the difference terms in Table 3, the phase RI values at 589 nm between the two techniques match to within ± 0.001 for three of the four lots tested and had comparable range and standard deviations of the individual RI measurements. One of the measurements shows a significant 0.0042 deviation. When reviewing the individual measurements for this data set (Table 4), the Abbe data showed significantly greater range and standard deviations for the five lenses, with the differences almost an order of magnitude greater than the data obtained using the GRI approach (standard deviations of 0.003 vs 0.0004). In fact, this detailed breakdown of

the individual measurement demonstrates that the GRI approach for finding the phase RI value is more indicative of the true final lens value than the value reported by the Abbe refractometer.

Table 4. Individual GRI-based and Abbe refractometer measurements for the lens data located in the 3rd row of Table 3.

	Measured	Abbe
Lens 1	1.40222	1.4005
Lens 2	1.40196	1.3962
Lens 3	1.40263	1.3944
Lens 4	1.40196	1.40143
Lens 5	1.40167	1.39673
Average	1.40209	1.39785
Std Dev	0.00036	0.00299
Min	1.40167	1.3944
Max	1.40263	1.40143
Max-Min	0.00096	0.00703

4.2.4. Senofilcon A and Senofilcon C at 543 nm

For silicone hydrogel contact lenses, the Abbe refractometer is not accurate or sensitive enough for practical measurements. However, extensive data for two silicone hydrogel materials, senofilcon A and C, has been obtained using many different known and internally-developed methods, direct and indirect. This data has led to the conventional values for RI at 543nm used for senofilcon A ($n=1.4216$) and senofilcon C ($n=1.4203$) used company-wide

Table 5 shows comparison between the measured RI values to the conventional historical values. The maximum deviation is -0.0020. Note, that the conventional RI value is set during material and design development, with the value not accounting for batch to batch reactive monomer mixture (RMM) tolerances or effects of the manufacturing process. The conventional documented RI value of silicon hydrogel materials have not been previously measured down to these precision levels, so the technique shown here is valuable not only in helping to achieve ISO 18369 tolerance levels, but also to monitor manufacturing and RMM influences on the final lens RI.

Table 5. Measured RI as compared to the standard RI for hydrogels.

Phase RI @ 543 nm			
Material	Measured RI	Historical RI	Difference RI (Measured Minus Historical)
Senofilcon A	1.4204	1.4216	-0.0012
Senofilcon A	1.4213	1.4216	-0.0003
Senofilcon A	1.4214	1.4216	-0.0002
Senofilcon A	1.4207	1.4216	-0.0009
Senofilcon C	1.4183	1.4203	-0.0020

4.3. Measurement sensitivity for phase RI

In the next set of experiments, we aim to answer the question of measurement precision – how small of a phase refractive index change can the developed GRI measurement instrument detect?

4.3.1. Different concentrations of saline solutions

A standard packing saline solution ($n = 1.3367$ @ 543 nm) was modified by evaporation or dilution to create 4 additional concentrations. The five concentrations were then measured using the SHR and using the GRI method to obtain phase RIs for 543.4, 546.1, 587.9, and 589.3 nm wavelengths, similar to the approach taken for Brix sucrose measurements above. The *deviations* from the RI of the standard concentration were then compared between the two methods (Table 6).

Table 6. Changes in the phase RI obtained using Schmidt-Haensch vs GRI technique for different saline solutions concentrations.

	Schmidt-Haensch				GRI to Phase RI Conversion			
	Difference from Standard Packing Solution RI				Difference from Standard Packing Solution RI			
Lambda (nm)	Salty 1	Salty 2	Diluted 1	Diluted 2	Salty 1	Salty 2	Diluted 1	Diluted 2
543.4	0.0013	0.0004	-0.0002	-0.0005	0.0014	0.0004	-0.0001	-0.0004
546.1	0.0013	0.0004	-0.0001	-0.0005	0.0014	0.0004	-0.0001	-0.0004
587.6	0.0013	0.0004	-0.0002	-0.0005	0.0014	0.0004	-0.0001	-0.0004
589.3	0.0014	0.0005	-0.0001	-0.0004	0.0014	0.0004	-0.0001	-0.0004

Table 6 shows that both the Schmidt-Haensch and the GRI approach can detect changes in phase RI at the ~ 0.0002 level and both agree in magnitude of the change. This serves as evidence that the GRI approach can detect changes that are meaningful to the in-solution to in-air conversion process at the required sensitivity level.

4.3.2. Correlation with the lens refractive power change

Three different batches of silicon hydrogel RMM (senofilcon A) were used to manufacture the same lens design and optical power on the same manufacturing line but at different times. The lenses were then measured on the proposed device and the phase RI value obtained using the GRI measurement approach, at 543 nm (Table 7).

Table 7. Silicon hydrogel lot-to-lot phase RI variations, as obtained using the GRI technique.

Lot ID	Phase RI @ 543 nm
23	1.4214
53	1.4207
59	1.4213
Average	1.4211
Max	1.4214
Min	1.4207
Range (max - min)	0.0007

The measured maximum shift of 0.0007, when used to calculate the refractive power of the lens using the thick lens equation and the conversion from in-solution measured power to in-air reported power, corresponds to an expected refractive power shift of 0.042 D.

These same lenses were then measured using a wavefront sensor and resulted in an average shift in optical power of 0.046 D between lots 23 and 53, giving excellent agreement between the measured shift in RI and the corresponding measured shift in optical power.

4.3.3. RI variations for lenses made using the same RMM batch

The same mixed senofilcon A RMM batch was used to manufacture four lenses with different optical powers on the same manufacturing line. It is therefore expected that these lenses should have the identical phase RI, although some variations are likely present due to the manufacturing process for lenses of different thicknesses and lens volumes. Table 8 shows the results of the phase RI measurements using the GRI approach, for 543 nm wavelength light.

Table 8. Phase RI measurement for the lenses manufactured from the same RMM batch.

	Phase RI @ 543 nm	Historical RI	Difference (Measured Minus Historical)
SKU 1	1.42152	1.4216	-0.00008
SKU2	1.42136	1.4216	-0.00024
SKU3	1.42127	1.4216	-0.00033
SKU4	1.42160	1.4216	0.00000
Average	1.42144	1.4216	-0.00016
Range (max-min)	0.00033		

The measurements show that the maximum difference between different Stock Keeping Units (SKUs, or prescriptions) is 0.00033. The measured values are also compared to the standard senofilcon lenses RI of 1.4216. Note that the data for this study was collected over four separate measurement days.

Figure 13 shows the variations in the measured phase RI for other wavelengths as well. The GRI system can therefore detect very subtle difference in RI between SKUs, with all four lots showing excellent agreement to the standard RI value for the material.

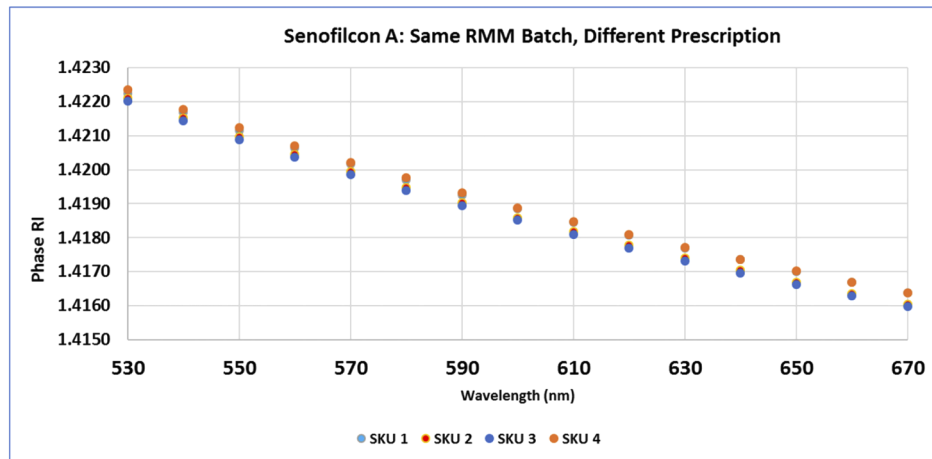


Fig. 13. Silicon hydrogel, SKU to SKU phase RI.

5. Proposed standardized measurement procedure

The described technique provides an opportunity for developing an alternative quality control procedure for obtaining refractive index. Most contact lens manufacturers may benefit from this procedure by improving measurement accuracy and through standardization of measurement procedures of contact lenses across companies and test laboratories.

The current standard procedure is to use the Abbe refractometer to measure six lenses, and to average these measurements to obtain a single RI value at 589 nm. This value is then converted to 543 nm wavelength, which is used for the JJVC wavefront sensor measurements. This conversion factor between wavelengths was established early in the wavefront sensors lifecycle using alternate refractometers, mainly based on liquid studies. This procedure, however, does not produce sufficiently accurate results and leads to significant challenges in quality control and to the difference in the outcomes for different manufacturers. Improving this procedure and the overall quality of ophthalmic optics is the primary motivation behind the work presented in this manuscript.

Based on the work and results obtained using the GRI measurement approach, we are proposing a different procedure as follows:

1. Measure GRI for a lot of 5 lenses at each wavelength from 530 nm to 670 nm in 10 nm steps,
2. Average the GRI values at each wavelength for all lenses
3. Fit the GRI dispersion curve with a Sellmeier equation
4. Apply the appropriate λ^* based on the assumed RI
5. Convert the GRI to phase RI
6. Fit the phase RI curve with a 2nd order polynomial to calculate phase RI at any wavelength from 530 to 670 nm

For Step 2, we have checked whether GRI measurements should be averaged and then converted to phase RI, or should the conversion take place first, and then the phase RI measurements averaged. We have tested five different lens designs and four different RMMs. The difference in the final phase RI values, obtained using the two different approaches, was insignificant in the 5th and 6th decimal place across the entire range of 530 nm to 670 nm.

6. Development plan / next steps

Additional development steps must be conducted by Lumetrics in order to offer the developed technique for use by manufacturing technicians.

6.1. Data confidence

The sample size of five lenses, chosen to conduct this work and to develop the test procedure in Section 5, was selected out of convenience to provide statistical evidence while at the same time keeping the development time at a reasonable level.

As more data is collected and the technique progresses through formal validation testing, the sample size will be more rigorously assessed to ensure it is adequate to detect the necessary shifts in RI – statistical rigor will be applied to sample size determinations.

For step 6 in Section 5, additional work is planned to determine whether using Sellmeier fit within this limited range of wavelengths will lead to an improvement in accuracy as compared to the 2nd order polynomial fit.

6.2. Additional wavelengths

Covering the range from 530 to 670 nm allows a determination of the phase dispersion curve at the wavelengths of interest, 543 nm and 589 nm, used for quality control testing of the manufactured contact lenses. One shortcoming of this range is that the Abbe number of the materials cannot be calculated, a value of interest to most lens designers. Additional development

will be aimed at including wavelengths in the blue range of the visible spectrum, to enable accurate RI measurement at 486.1 nm (c.f. instead of extrapolation).

6.3. Process time and automation

For the system to be used on a production scale, simplifications and automation must be introduced to enable operator-level function. Currently, the measurement process and data handling and analysis require approximately 3.5 hours for 5 lenses.

A joint development project between Lumetrics and JJVC is underway to build a production-ready quality control instrument based on the GRI prototype system described in this manuscript. It is expected that the automation will reduce the measurement process time by more than a factor of 2.

6.4. Cost reduction

The current SCLS-based measurement system represents a significant capital investment, that can reach several hundreds of thousands of dollars, where multiple units may be cost prohibitive to all but the largest contact lenses manufacturers. The most expensive component of the system is the tunable SCLS. To address this hurdle, a simplified device is under development by Lumetrics, utilizing a single wavelength in the visible range, 650 nm. This simplified system will serve a complementary role to the more comprehensive multi-wavelength system. The comprehensive system can be used in early material or process development to set the true RI standards at the wavelength(s) of interest, while the single-wavelength system will be used for larger scale monitoring to detect changes in the final lens RI, as a more user-friendly and faster measurement system for production support. Likely a conversion factor will have to be developed between the two systems due to the difference in the spectral properties between the two system types.

7. Summary

Accurate refractive index knowledge of soft contact lenses is critical for lens performance evaluation. Current measurement techniques are problematic due to lens geometry, hydration, lens chemistry and material composition. The proposed measurement equipment and technique will allow the bulk material phase RI characterization at visible wavelengths with accuracy of ± 0.001 and sensitivity at the 0.0002 level.

Disclosures

TS and XW: Johnson and Johnson Vision care, Inc (E); DG: Lumetrics, Inc (E, P), FI: Lumetrics, Inc (I, E, P).

References

1. *ISO 18369-1 Ophthalmic optics - contact lenses. Parts 1-4*, Geneva: International Organization for Standardization, 2017.
2. E. P. Goodwin, "PhD Thesis: Dual interferometer system for measuring index of refraction," The University of Arizona, Tucson, AZ.
3. M. A. Marcus, D. S. Gibson, K. J. Hadcock, and F. V. Ignatovich. US Patent 10,190,977, 2019.
4. J. R. Rogers and M. D. Hopler, "Conversion of group refractive index to phase refractive index," *J. Opt. Soc. Am. A* **5**(10), 1595–1600 (1988).
5. H. Maruyama, T. Mitsuyama, M. Ohmi, and M. Haruna, "Simultaneous measurement of refractive index and thickness by low-coherence interferometry considering chromatic dispersion of index," *Opt. Rev.* **7**(5), 468–472 (2000).
6. S. Kim, J. Na, M. J. Kim, and B. H. Lee, "Simultaneous measurement of refractive index and thickness by combining low-coherence interferometry and confocal optics," *Opt. Express* **16**(8), 5516–5526 (2008).
7. J. Yao, J. Huang, P. Meemon, M. Ponting, and J. P. Rolland, "Simultaneous estimation of thickness and refractive index of layered gradient refractive index optics using a hybrid confocal-scan swept-source optical coherence tomography system," *Opt. Express* **23**(23), 30149–30164 (2015).

8. M. R. Hee, "Optical coherence tomography: theory," in *Handbook of Optical Coherence*, (Marcel Dekker, New York, 2002), pp. 41–66.
9. S. Aumann, S. Donner, J. Fischer, and F. Muller, "Optical Coherence Tomography (OCT): Principle and Technical Realization," in *High Resolution Imaging in Microscopy and Ophthalmology*, (Springer, Cham, 2019), pp. 59–87.
10. C. K. Hitzenberger, "Measurement of corneal thickness by low-coherence interferometry," *Appl. Opt.* **31**(31), 6637–6642 (1992).
11. A. F. Fercher, W. Drexler, C. K. Hitzenberger, and T. Lasser, "Optical coherence tomography - principles and applications," *Rep. Prog. Phys.* **66**(2), 239–303 (2003).
12. C. J. Ditchman, C. Cotton, and D. W. Diehl, "Surface and thickness metrology using scanning low-coherence dual interferometry (SLCDI)," in *SPIE OptiFab*, (Optifab, Rochester, NY, 2007).
13. T. Blalock and S. Heveron-Smith, "Practical applications in film and optics measurements for dual-lightsource interferometry," in *SPIE Optics East*, (Optics East, Philadelphia, PA, 2004).
14. M. A. Marcus, S. Gross, and D. C. Wideman, "Associated dual interferometric measurement method for determining a physical property of an object," US Patent 5,96,09, 1997.
15. P. E. Ciddor, "Refractive index of air: new equations for the visible and near infrared," *Appl. Opt.* **35**(9), 1566–1573 (1996).
16. H. A. Buchdahl, *Optical Aberration Coefficients*, (Dover, New York, 1968), pp. 150–154.
17. G. Forbes, "Chromatic coordinates in aberration theory," *J. Opt. Soc. Am. A* **1**(4), 344–349 (1984).
18. M. Born and E. Wolf, *Principles of Optics: Electromagnetic Theory of Propagation, Interference and Diffraction of Light*, (Elsevier, 2013).
19. M. Daimon and A. Masumura, "Measurement of the refractive index of distilled water from the near-infrared region to the ultraviolet region," *Appl. Opt.* **46**(18), 3811–3820 (2007).
20. I. H. Malitson, "Interspecimen comparison of the refractive index of fused silica," *J. Opt. Soc. Am.* **55**(10), 1205–1208 (1965).
21. *SCHOTT Zemax catalog*, Schott, Inc, 2017.
22. J. Rheims, J. Koser, and T. Wriedt, "Refractive-index measurements in the near-IR using an Abbe refractometer," *Meas. Sci. Technol.* **8**(6), 601–605 (1997).
23. "ATR-L refractometer," Schmidt Haensch, Inc, [Online]. Available: <https://schmidt-haensch.com/products/laboratory-instruments/refractometer/atr-l/>. [Accessed 12 12 2019].